YAP/TAZ-Inhibitor-Based Drug Delivery System for Cancer Therapy

by

Ziqian Zhang

BS, Sun Yat-sen University, 2018

Submitted to the Graduate Faculty of

School of Pharmacy

of the requirements for the degree of

Master of Science

University of Pittsburgh

2020

UNIVERSITY OF PITTSBURGH

SCHOOL OF PHARMACY

This thesis/dissertation was presented

by

Ziqian Zhang

It was defended on

April 3, 2020

and approved by

Song Li, Professor, Department of Pharmaceutical Science

Vinayak Sant, Assistant Professor, Department of Pharmaceutical Science

Junmei Wang, Associate Professor, Department of Pharmaceutical Science

Da Yang, Assistant Professor, Department of Pharmaceutical Science

Thesis Advisor/Dissertation Director: Song Li, Professor, Department of Pharmaceutical
Science

YAP/TAZ-Inhibitor-Based Drug Delivery System for Cancer Therapy

Ziqian Zhang, BS

The YES-associated protein (YAP) and the transcriptional co-activator with PDZ-binding motif (TAZ) are two important transcriptional co-activators in the Hippo signaling pathway, which play an essential role in organ size control, tumor suppression, tissue regeneration and stem cell self-renewal. However, aberrant activation of YAP and TAZ due to deregulation of the Hippo pathway or overexpression of YAP/TAZ and TEADs can promote cancer development. Hence, pharmacological inhibition of YAP and TAZ may be a useful approach to treat tumors with high YAP/TAZ activity. Here, we developed a YAP/TAZ-inhibitor (niflumic acid (NA))-based drug delivery system for enhanced cancer therapy. Through disrupting the interaction between the TEA domain transcription factors (TEADs) and YAP/TAZ, NA reduces the expression of downstream genes that promote tumor proliferation and migration. At the same time, other hydrophobic anti-cancer drug can be co-delivered to tumor site to improve the overall antitumor activity and decrease side effect. Our strategy may not only improve delivery of well-established anti-cancer drugs, but also further improve their efficacy through inhibiting YAP/TAZ activity.

Table of Contents

List of Tables

List of Figures

Preface

I would like to thank my advisor, Dr. Song Li, for his help in this project and the writing of this thesis. I would like to thank other members in or was in Dr. Song Li's lab, including Yixian Huang, Jingjing Sun, Yue Zhang, Weina Ma, Guolian Ren, Jieni Xu, Zhuoya Wan, Zhangyi Luo, Haozhe Huang, Yuang Chen, Bei Zhang, Apurva Pardeshi, Dingwei Diao, Pengfei Ren and Chaogang Wei for their help in my research. I would like to thank my committee members, Dr. Song Li, Dr. Vinayak Sant, Dr. Junmei Wang and Dr. Da Yang for their suggestions and comments. I would like to thank all other students and faculties in the center of Pharmacogenetics, school of Pharmacy, University of Pittsburgh who supported me in all ways, especially Dr. Maggie Folan, Dr. Samuel M. Poloyac and Lori M. Altenbaugh. Last, I would like to thank my family and friends for their company and support, which enable me to chase for my MS degree. Thank you all very much.

1.0 Introduction

1.1 The Hippo signaling pathway

The Hippo signaling pathway is an evolutionarily conserved signaling pathway which plays an important function in organ size control, tissue regeneration, as well as tumor suppression[1-3]. Initially discovered in *Drosophila melanogaster*, the Hippo pathway was found to be an important regulator of tissue growth[4-6]. Later, the Hippo pathway was found to be highly conserved from *Drosophila* to mammals with similar function[4, 7]. In mammals, it is consisted of a serine/threonine kinase cascade and transcriptional co-activators Yes-associated protein (YAP) and its paralog transcriptional activator with PDZ-binding domain (TAZ). The core kinases involved in the kinase cascade include mammalian STE20-like kinases (MST1/2) and large tumor suppressor kinases (LATS1/2). When activated, MST1/2 form complexes with adaptor protein Salvador Homolog (SAV1) and phosphorylate LATS1/2 and their adaptor protein Mob1 Homolog (MOB1) for activation[8-10]. Then LATS1/2 form complexes with MOB1 and further phosphorylate YAP/TAZ, leading to their cytoplasmic sequestration via binding to 14-3-3 or ubiquitinoylation, and degradation[11-15]. As a result, YAP/TAZ are inhibited when the Hippo pathway is turned on. In contrast, when the Hippo pathway is not active, unphosphorylated YAP/TAZ accumulate in the nucleus and promote expression of target genes mainly with the help of TEAD family transcription factors[16, 17]. The transcriptional activity of YAP/TAZ is dependent on their interactions with TEAD since they do not contain a DNA-binding domain[18, 19].

1.2 Hippo signaling and cancer

Numerous evidences show that the Hippo pathway is highly related to development of a broad range of cancers[3]. At cellular level, the Hippo pathway responds to many cellular events including apicobasal polarity, mechanotransduction, cell-cell adhesion and contact inhibition to regulate the activity of YAP/TAZ, and thus the expression of genes involved in cell proliferation, cell survival, cell competition and stem cell maintenance[4]. It has been shown that disruption of the Hippo signaling or over-activation of YAP/TAZ will cause this program to lose control, which is sufficient to drive tumorigenesis[2, 20]. For example, knockout of MST1 and MST2 in the mouse liver was shown to promote tumor formation in mice[20]. Furthermore, the overexpression of YAZ/TAZ has been shown to enhance anoikis resistance, epithelial-to-mesenchymal transition (EMT), drug resistance and metastasis[2, 12, 21-24]. In summary, many studies strongly support an oncogenic role for YAP/TAZ and a tumor-suppressive function for Hippo pathway upstream components. Moreover, it has been reported that the deregulation of the Hippo pathway happens frequently in a broad range of human cancers like lung cancer, ovarian cancer, liver cancer and breast cancer, correlating with poor patient prognosis[25]. All these researches suggest Hippo pathway as a promising target for cancer therapy.

1.3 Pharmacologic manipulation of the Hippo signaling pathway by NA

Although the important role of Hippo pathway in cancer has been well documented, targeting this pathway for cancer therapy still presents challenges. There are several upstream regulators in the Hippo signaling pathway. In addition, there are some crosstalk between Hippo and other signaling pathways, suggesting that disruption of

the Hippo pathway or its crosstalk with other signal pathways might be a possible strategy to regulate the activity of YAP/TAZ[26].

However, as diverse cellular signals regulate YAP/TAZ nucleocytoplasmic transport, it is unclear whether these compounds could be effective in treating cancers caused by a defective Hippo pathway. And as these regulator proteins are also involved in other important cellular signaling networks, side effect is probably unavoidable. Therefore, drugs that directly regulate the Hippo pathway might represent a more promising approach. An ideal target for small molecule therapeutics is protein kinases that function as oncogenes. But unfortunately, the Hippo pathway kinases, MST1/2 and LATS 1/2 are tumor suppressors[11]. Because small molecule activators are hardly available, they are not suitable for drug targeting. Ruling out these possibilities, the most attractive therapeutic targets are the key transcriptional co-activators YAP/TAZ as the final common conduits of this pathway.

Niflumic acid (NA), an inhibitor of YAP/TAZ, was reported to be able to bind to YAP-binding domain on TEAD with a high affinity[27]. Because YAP/TAZ relies on TEADs for activating gene expression, inhibiting the oncogenic activities of YAP/TAZ can be achieved by directly targeting TEAD-YAP protein-protein interactions[28]. Although NA does not affect the binding of TEAD to YAP peptide, significant reduction in the TEAD reporter activity was observed. And after NA treatment, proliferation and migration of cells decrease significantly[27]. These results indicated that NA is an effective inhibitor of YAP/TAZ. However, a short half-life of 2.5 h in blood and poor tumor distribution greatly limit its application for *in vivo* study[29].

1.4 POEG-b-PNA is an ideal carrier to co-deliver NA and other anti-cancer drugs for targeted cancer therapy

In order to investigate whether inhibition of YAP/TAZ could be a promising approach to treat tumors with high YAP/TAZ activity and enhance tumor therapy in combination with other anti-tumor drugs, we have developed a novel NA prodrug micellar formulation to co-deliver NA and other anti-tumor drugs. The prodrug nanocarrier is based on a well-defined poly-(oligo ethylene glycol)-co-poly-(niflumic acid (4-vinylbenzyl) ester) (POEG-b-PNA) di-block copolymer, which can self-assemble to form micelles for drug delivery. We hypothesize that this nanoparticle can accumulate at tumor site and slowly release NA. In addition, POEG-b-PNA is capable of co-delivering another anticancer drug to improve the overall antitumor activity while reducing drug-associated side effect.

2.0 Methods

2.1 Materials

Dasatinib, gefitinib, sunitinib and doxorubicin·HCl were purchased from LC Laboratories. 4-Cyano-4-pentanoic acid, niflumic acid, vinylbenzyl chloride (VBC) monomer, potassium carbonate, oligo(ethylene glycol) methacrylate (average $Mn = 500$, OEG500), 2- Azobis(isobutyronitrile) (AIBN), trypsin-EDTA solution, 3-(4,5-dimethylthiazol-2-yl)-2,5- diphenyl tetrazolium bromide (MTT) and Dulbecco's Modified Eagle's Medium (DMEM) were purchased from Sigma-Aldrich (MO, U.S.A). AIBN was purified by recrystallization in anhydrous ethanol. Fetal bovine serum (FBS), penicillin-streptomycin solution, Lipofectamine 2000 and TRIzol lysis reagent were purchased from Invitrogen (NY, U.S.A.). QuantiTect Reverse Transcription Kit was purchased from Qiagen (MD, U.S.A). All solvents used in this study were HPLC grade. Antibody against YAP was purchased from Cell Signaling Technology, Inc. (MA, USA). SuperSignalTM West Fento Maximum Sensitivity Substrate Kit and PierceTM RIPA buffer were purchased from Thermo Scientific (MA, USA). pCMV-β-galactosidase plasmid was obtained from Clontech (Mountain View, CA, USA).

2.2 Synthesis of niflumic acid monomer

4-vinylbenzyl chloride (0.60 g, 4 mmol), niflumic acid (1.13 g, 4 mmol), Potassium carbonate (2.76 g, 20 mmol) and were mixed in 20 ml N,N-Dimethylformamide and reacted at 50 °C under stirring. After 6 h, cooled down the mixture and added 200 ml dichloromethane to extract the product. Then centrifuged the mixture at 4500 rpm for

10 min. The participate was washed with methylene dichloride for two times and all the supernatant was collected, washed by water for three times. Anhydrous sodium sulphate was added later for dehydration. Niflumic acid monomer was purified by silica gel column chromatography using dichloromethane/hexane (v/v=1/3 to 1/1) as the elution buffer.

2.3 Synthesis of POEG-b-PNA polymer

Niflumic acid monomer (200 mg, 0.5 mmol), OEG500 monomer (450 mg, 0.9 mmol), 4-Cyano-4-(thiobenzoylthio)pentanoic acid (8.4 mg, 0.03 mmol) and azobisisobutyronitrile (1.64 mg, 0.01 mmol) were dissolved in anhydrous tetrahydrofuran (2.0 ml) and added into a Schlenk tube. After three free-pump-thawing cycles, the mixture was filled with N_2 and immersed into an oil bath thermostated at 80 °C for polymerization. After 24 h, quenched the reaction by immersing the tube into liquid nitrogen and participated the mixture in diethyl ester for three times. The POEG-b-PNA polymer was obtained after vacuum drying. Conversion of PNA monomer was 85% and conversion of OEG500 monomer was 67%.

2.4 Characterization of the synthesized monomer and polymer

^{1}H NMR spectrum was examined on a Varian-400 FT-NMR spectrometer at 400.0 MHz with $CDCl_3$ as the solvent.

2.5 Preparation and characterization of blank and drug-loaded POEG-b-PNA micelles

Dasatinib, doxorubicin, sunitinib or gefitinib solution (1mg/mL in methylene chloride/methanol (v/v=1/1)) was mixed with POEG-b-PNA polymers (20 mg/mL in methylene chloride) at different carrier/drug weight ratios. The solvent was removed by nitrogen flow to produce a thin film of carrier/drug mixture, which was further dried in vacuum for 2 h to remove any remaining solvent. Then the thin film was hydrated and gently vortexed in PBS to form dasatinib-loaded POEG-b-PNA micelles.

The size distribution and zeta potential of blank and drug-loaded micelles were examined by dynamic light scattering (DLS) through a Malvern Zeta Nanosizer.

2.6 Critical micelle concentration (CMC) of POEG-b-PNA micelles

The CMC values of POEG-b-PNA micelles were determined by fluorescence measurement using Nile red as a fluorescence probe. Briefly, Nile red dissolved in DCM was added to test-tubes and the solvent was evaporated at room temperature. POEG-b-PNA micelles ranging from 1.0×10^{-4} to 5×10^{-1} mg/mL were then added into Nile red. The final concentration of Nile red was kept at 6.0×10^{-7} M. The micelles were kept overnight to allow the solubilization equilibrium of Nile red. Excitation was carried out at 550 nm and emission spectra were recorded from 570 to 720 nm. The CMC value was determined as the cross-point when extrapolating the intensity at low and high concentration regions.

2.7 Cell culture

4T1.2 is a mouse metastatic breast cancer cell line. This type of cell was cultured in DMEM culture medium with 10% (v/v) fetal bovine serum and 100 IU/mL penicillin and 100 μg/mL streptomycin at 37 °C in a humidified 5% CO2-95% air atmosphere. 4T1.2 cell line used in this work was obtained from ATCC (VA. U.S.A).

2.8 Animals

Female BALB/c mice, 6-8 weeks in age, were purchased from Charles River (Davis, CA). All animals were housed under pathogen-free conditions according to AAALAC guidelines. All animal-related experiments were performed in full compliance with institutional guidelines and approved by the Animal Use and Care Administrative Advisory Committee at the University of Pittsburgh.

2.9 In vitro cytotoxicity assay

Cytotoxicity assay was performed on 4T1.2 mouse breast cancer cell line. Cells were seeded in 96-well plates at a density of 1.5×10^3 cells/well and incubated 24 h as described previously to allow cell attachment.

To evaluate the combinational effect of NA and other anti-cancer drugs, cells were treated with various concentrations of free NA, free dasatinib, and the combination of both respectively for 48 h. To examine the cytotoxicity of drug-loaded POEG-b-PNA micelles, free dasatinib, blank POEG-b-PNA and dasatinib/POEG-b-PNA (w/w ratio

9

POEG-b-PNA: dasatinib=40: 1) were incubated with cells for 48h before MTT assay was performed.

MTT assay and the calculation of cell viability were performed as described before. The anti-proliferation data for single drug and combination treatment were fitted to an inhibitory, normalized dose-response model with variable slope (Y = 100/ (1 + 10^((LogEC50-X) *Hillslope). (GraphPad Prism, San Diego, CA)

2.10 Real-time PCR

Real-time PCR studies were performed on 4T1.2 mouse breast cancer cell line. 4T1.2 (2×10^4 cells/well) was seeded in 6-well plates followed by 24 h of incubation in DMEM containing 10% FBS and 1% streptomycin/penicillin. After 24 hours, medium was replaced with medium with 2% FBS containing free NA. After 48 hours, total cellular RNA was extracted using the TRIzol lysis reagent. cDNA was generated from the purified RNA using QuantiTect Reverse Transcription Kit following to the manufacturer's instructions. The cDNAs corresponding to different genes examined were amplified by PCR using the specific primers respectively. (supplementary form) Quantitative real-time PCR was performed using SYBR Green Mix on a 7900HT Fast Real-time PCR System. Relative target mRNA levels were analyzed using delta-delta-Ct calculations and normalized to GAPDH.

2.11 Western blot

Western blotting was performed to evaluate the YAP level in MDA-MB 4T1.2 cell line. Cells grown in six-wells plates with 80% confluency were treated with free NA for 24 h. Cells were washed twice with pre-cooled PBS and lysed in PierceTM RIPA buffer for 40 min in 4℃. Protein concentrations were determined by BCA method, and equal amounts of total protein lysate were resolved on a 10% SDS-PAGE and subsequently transferred to a nitrocellulose membrane. Membranes were blocked with 5% nonfat milk in PBS for 1 h prior to incubation with rabbit anti-YAP primary antibody dissolved in PBST (DPBS with 0.1% Tween 20) overnight at 4 °C. The blots were washed with PBST and then probed with goat antirabbit IgG for 1 h at room temperature followed by chemiluminescence detection by SuperSignalTM West Fento Maximum Sensitivity Substrate. GAPDH was used as a loading control.

2.12 Cell transient transfection and luciferase reporter assay

4T1.2 cells were cultured as previously described. TEAD activity reporter developed by Dupont et al. was used in the assay[30]. Cells in a 48-wells plate were transfected with 500 ng of TEAD firefly luciferase and 250 ng of CMV-β-galactosidase constructs using a Lipofectamine 2000-mediated method. After 24 h, the cells were incubated with different concentration of NA for another 24 h before luciferase or β-gal activity assay. The luciferase activity was determined using luciferin as substrate and was normalized against the co-transfected β-galactosidase activity.

2.13 In vivo biodistribution with near-infrared fluorescence imaging

DiR-loaded POEG-b-PNA micelles were prepared similarly to dasatinib-loaded POEG-b-PNA micelles at a POEG-b-PNA to DiR ratio of 80/1 (w/w). DiR-loaded POEG-b-PNA micelles were injected to 4T1 tumor bearing mice at a DiR dose of 2.5 mg/kg. At 1,6,12,24,48 and 72 hours, the mice were imaged by IVIS 200 system (Perkin Elmer, USA) at a 0.5s exposure time with excitation at 730 nm and emission at 835nm. The mice were then sacrificed and perfused. Then major organs were dissected and subjected to ex vivo imaging.

3.0 Results

3.1 *In vitro* YAP inhibition effect of NA in 4T1.2 breast cancer cells

The expression of YAP in 4T1.2 murine breast cancer cells was first confirmed by western blot (Fig. 1A). 4T1.2 showed a high YAP expression, which is consistent with previous report, indicating that YAP is highly activated in this cell line and 4T1.2 is an ideal model for YAP study. It has been previously reported that NA could inhibit TEAD-YAP activity by targeting the YAP-binding pocket of TEAD in human HEK-293 cell line. However, this inhibition might be different in murine cells due to the difference in protein structure. Therefore, the inhibition effect of NA on 4T1.2 cell line was first investigated. After treated with NA, the protein level of YAP in 4T1.2 cells showed no significant difference compared to untreated cells (Fig. 1A). However, the mRNA expression levels of YAP target genes such as *Ctgf*, *Cyr61* and *Amolt2* genes [16] were dramatically decreased after NA treatment (Fig. 1C). These data suggest that NA inhibited the YAP activity though it had no significant effect on its expression at protein level. We then went on to examine the YAP activity after NA treatment using a YAP luciferase reporter assay (Fig. 1B). Briefly, 4T1.2 cells were first transfected with a luciferase reporter in which the luciferase expression is under the regulation of a YAP-responsive promoter. Then, the luciferase activity was detected in 4T1.2 cells treated with free DMSO or various concentrations of NA. The signals were found to decrease in a dose-dependent manner after NA treatment, indicating that YAP activity was inhibited by NA. These data proved that NA can also serve as a YAP inhibitor on murine 4T1.2 breast cancer cell line, possibly by binding to the YAP-binding pocket on TEAD to suppress the TEAD-YAP activity, a similar mechanism reported for HEK293 cell line[27].

13
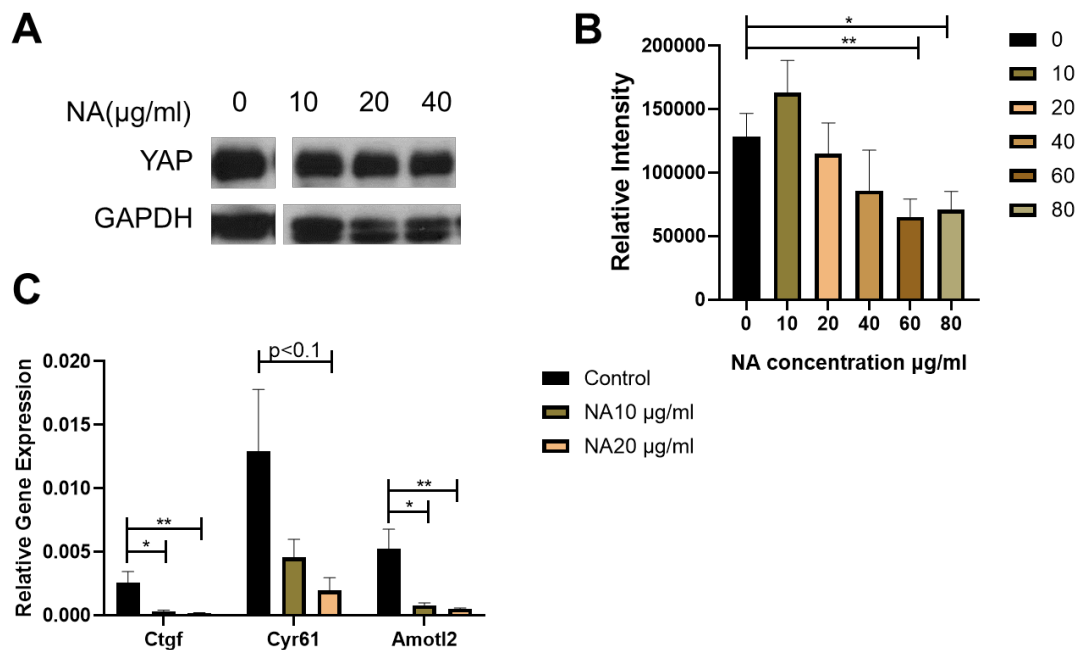
Figure 1 NA inhibit YAP activity in 4T1.2 breast cancer cells.

4T1.2 cells were treated with DMSO or variant concentration of NA in DMSO. (A) YAP protein levels were investigated by western blot. (B) YAP activities were detected using a luciferase reporter. Before NA treatment, cells were co-transfected with luciferase reporter plasmid and CMV-β-galactosidase plasmid. The fluorescent intensities were normalized by β-galactosidase activity. (C) Expression of three different YAP target genes- Ctgf, Cyr61 and Amotl2- were tested by qPCR and were normalized by expression level of GAPDH. Data are presented as the means ± SD for triplicate samples. P values were generated by student t-test for comparisons. *P < 0.05, **P < 0.01 (vs control).

3.2 Synthesis and characterization of POEG-b-PNA polymer

To improve the pharmacokinetics profile and the therapeutic effect of NA, a NA-based polymer was developed. In addition to improved delivery of NA itself, POEG-b-PNA can form a carrier to further facilitate codelivery of another anticancer drug. The POEG-b-PNA polymer was synthesized following the scheme depicted in Fig. 2. First,

NA monomer was synthesized via reaction of NA with 4-vinylbenzyl chloride. Then, POEG-b-PNA polymer was synthesized with NA monomer and OEG500 monomer via reversible addition-fragmentation transfer (RAFT) polymerization as reported previously[31].

The structures of NA monomer and POEG-b-PNA polymer were confirmed by H[1]NMR (Fig. 3A-B). The average numbers of NA unit and OEG500 unit in each POEG-b-PNA molecule were about 14 and 16, respectively. The average molecular weight of POEG-b-PNA polymer was about 13350 g/mol, calculated by NMR.

Blank POEG-b-PNA micelles and drug-loaded POEG-b-PNA were prepared by a film hydration method. The CMC value of POEG-b-PNA micelle was about 7.9 μg/ml (Fig. 4B), measured by using Nile red as a fluorescence probe. The relatively low CMC value of this polymer suggests a good stability following i.v. injection and dilution in blood, which can help to prevent the burst release of drug. The hydrodynamic size of POEG-b-PNA micelle was measured by dynamic light scattering method and the size distribution is shown in Fig. 4A. The size of POEG-b-PNA polymer is around 15.71 nm, while loading of dasatinib, doxorubicin, sunitinib or gefitinib had minimal impact on the particle size (Table 1). All these drugs can be loaded into POEG-b-PNA micelles at a drug/carrier weight ratio up to 1/10, and these drug-loaded micelles were stable in room temperature for two days with unchanged size distribution and clear solution.
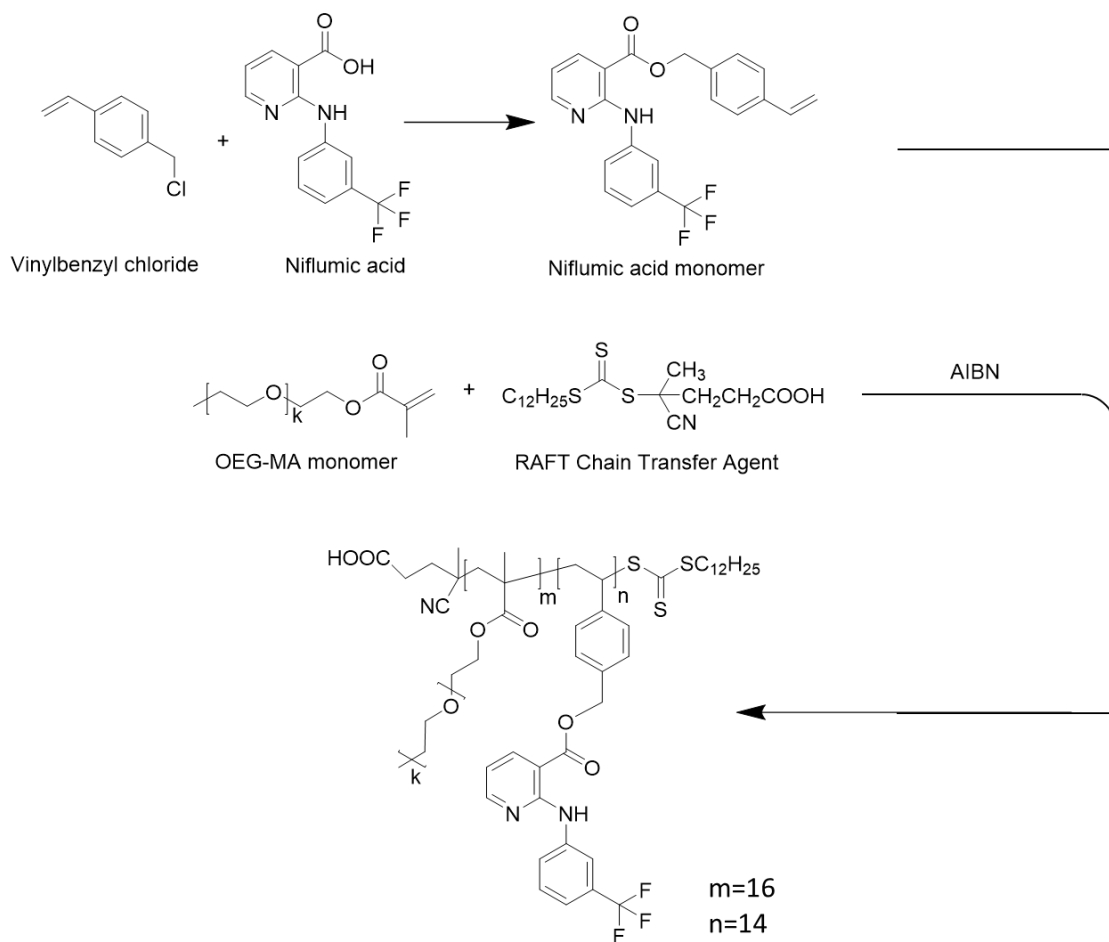
Figure 2 Synthesis Scheme of POEG-b-PNA Conjugate

NA was first linked to vinylbenzyl chloride via an ester bond to build NA monomer. Then POEG-b-PNA polymer was synthesized by NA monomer and OEG500 monomer via reversible addition-fragmentation transfer (RAFT) polymerization. The molecular weight and numbers of monomer units were adjusted by controlling input ratio among RAFT chain transfer agent, NA monomer and OEG-MA monomer.
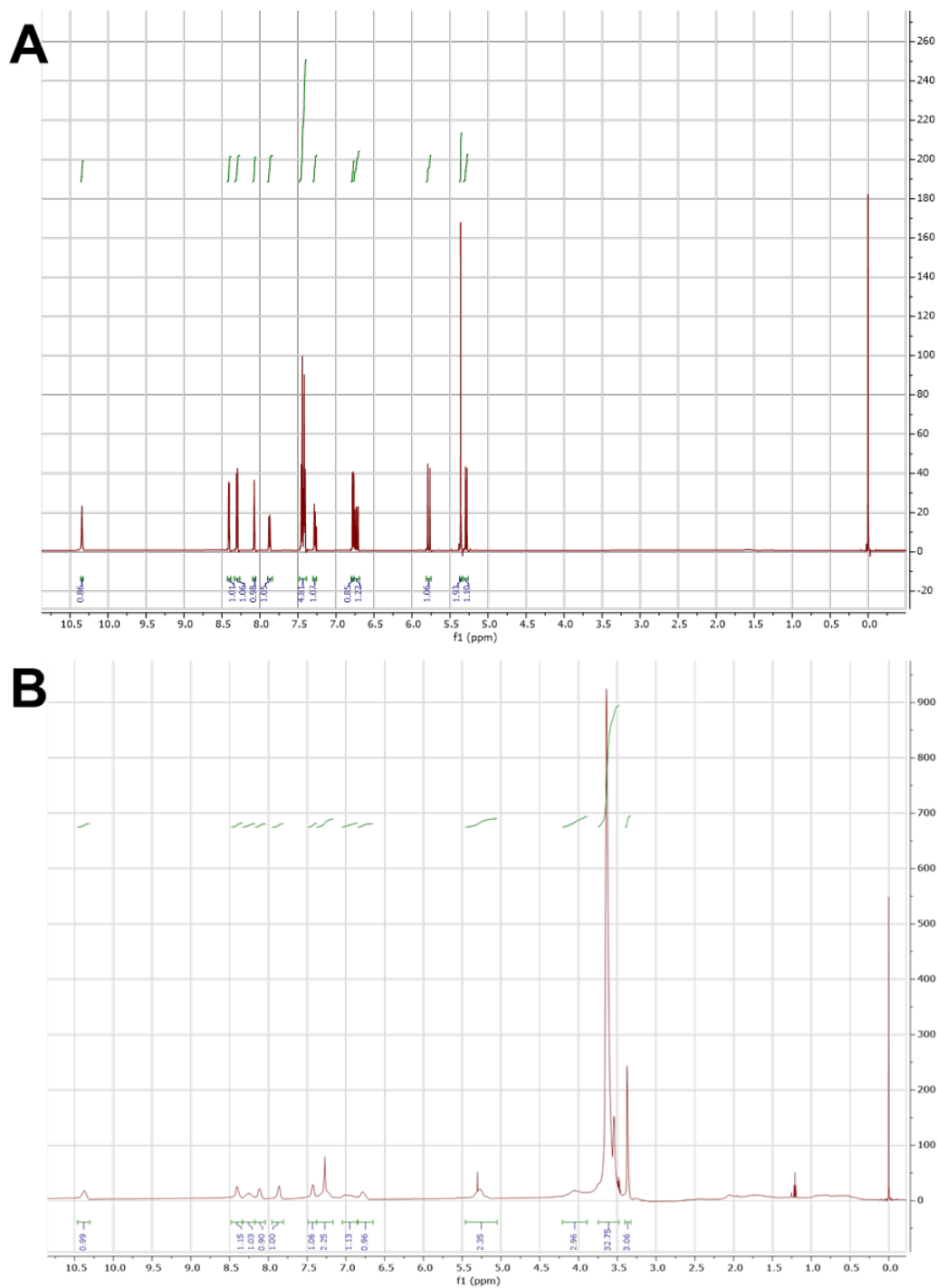
**Figure 3 ^{1}H-NMR of NA monomer and POEG-b-PNA conjugate**

NA monomer (A) and POEG-b-PNA (B) were dissolved in CDCl₃ for ^{1}H-NMR and the structures were confirmed. The numbers of NA monomer units and POEG-b-PNA units were calculated according to the integration area of their exclusive peaks. The average numbers of NA unit and OEG500 unit in each POEG-b-PNA molecule were about 14 and 16, respectively.
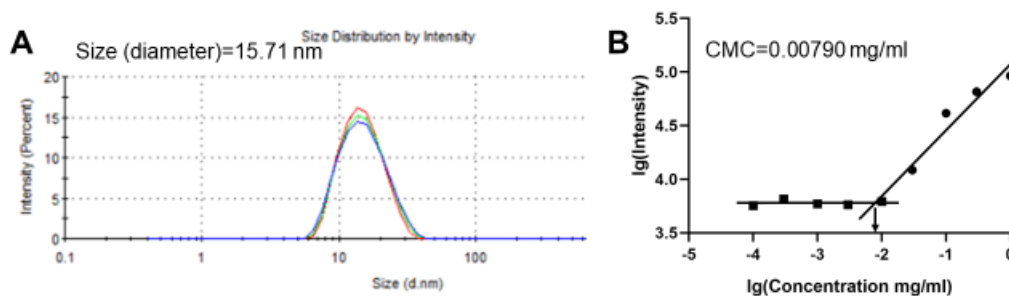
Figure 4 Size distribution and critical micelle concentration of POEG-b-PNA micelles

POEG-b-PNA micelles were prepared by simple film hydration method. POEG-b-PNA polymers were first dissolved in methylene chloride. The solvent was removed by nitrogen flow to produce a thin film. Then the thin film was hydrated and gently vortexed in PBS to form POEG-b-PNA micelles. The size distribution of these micelles was characterized by DLS, showing an average diameter size of 15.71 nm (A). Tests were run for three times. Critical micelle concentration was measured using Nile red (B). POEG-b-PNA micelles solution was diluted to different concentration and incubated with hydrophobic nile red dye. Then the supernatants were tested for fluorescent signals. Two lines were fitted as shown. The cross point of these two lines indicates a CMC of 7.9 μg/ml.

Table 1 Characterization of drug-loading POEG-b-PNA micelles

Drugs	Drug Loading Capacity (w/w)	Size	Stability (RT)
Gefitinib	1/10	Size=14.68 nm PDI=0.279	Over 48 h
Dasatinib	1/10	Size=14.14 nm PDI=0.168	Over 48 h
Sunitinib	1/15	Size=14.01 nm PDI=0.282	Over 48 h

		Size=13.67 nm	
Doxorubicin	1/15	PDI=0.314	Over 48 h

Drugs were first mixed with POEG-b-PNA polymer in dichloromethane/methanol (v/v=1/1) in different weight ratio. Then drug-loading micelles were prepared by film hydration method and their size distribution were measured by DLS. Samples with clear solution, unobservable precipitate and stable size were considered to load drug well. All samples were kept in room temperature for 2 days to follow their changes.

3.3 Synergistic effect of NA and other anti-cancer drugs on cancer cell proliferation

Since YAP has been reported to be overexpressed in many kinds of cancer cells[25], including drug-resistant cancer cells[32-34], it would be interesting to test whether inhibition of YAP by NA can sensitize cancer cells to other therapies including chemotherapy. Here, doxorubicin, sunitinib, gefitinib and dasatinib were selected to investigate their synergistic effect with NA on YAP-overexpressing 4T1.2 cell line. The proliferation inhibitory activity of doxorubicin, sunitinib, gefitinib and dasatinib, alone or in combination with NA, was examined on 4T1.2 breast cancer cell line via MTT assay. As shown in Fig. 5A, dasatinib or NA alone showed a concentration-dependent inhibition of proliferation on 4T1.2 cells. Combination of both led to an improvement in efficacy. A similar improvement in inhibition of cell proliferation was observed when NA was combined with doxorubicin (Fig. 5B), sunitinib (Fig. 5C), or gefitinib (Fig. 5D). To further assess the potential synergistic effect between NA and the four anti-cancer drugs, combination index was then calculated through the equation: $CI = (d1/IC_{50}1) + (d2/IC_{50}2)$. In this equation, d1 is the concentration of the first drug (NA)

required to achieve 50% inhibitory effect in combination treatment and $IC_{50}1$ is the IC_{50} value of the first drug (NA), while d2 is the concentration of the second drug (dasatinib, doxorubicin, sunitinib or gefitinib, respectively) required to achieve 50% inhibitory effect in combination treatment and $IC_{50}2$ means the IC_{50} value of the second drug (dasatinib, doxorubicin, sunitinib or gefitinib, respectively). The CI values of all tested drugs were shown in Table 2. Dasatinib and gefitinib showed a CI value significantly less than 1, indicating that they have synergistic effect in combination with NA. No synergy was found between NA and sunitinib or doxorubicin, with a CI value close to 1 or above 1.
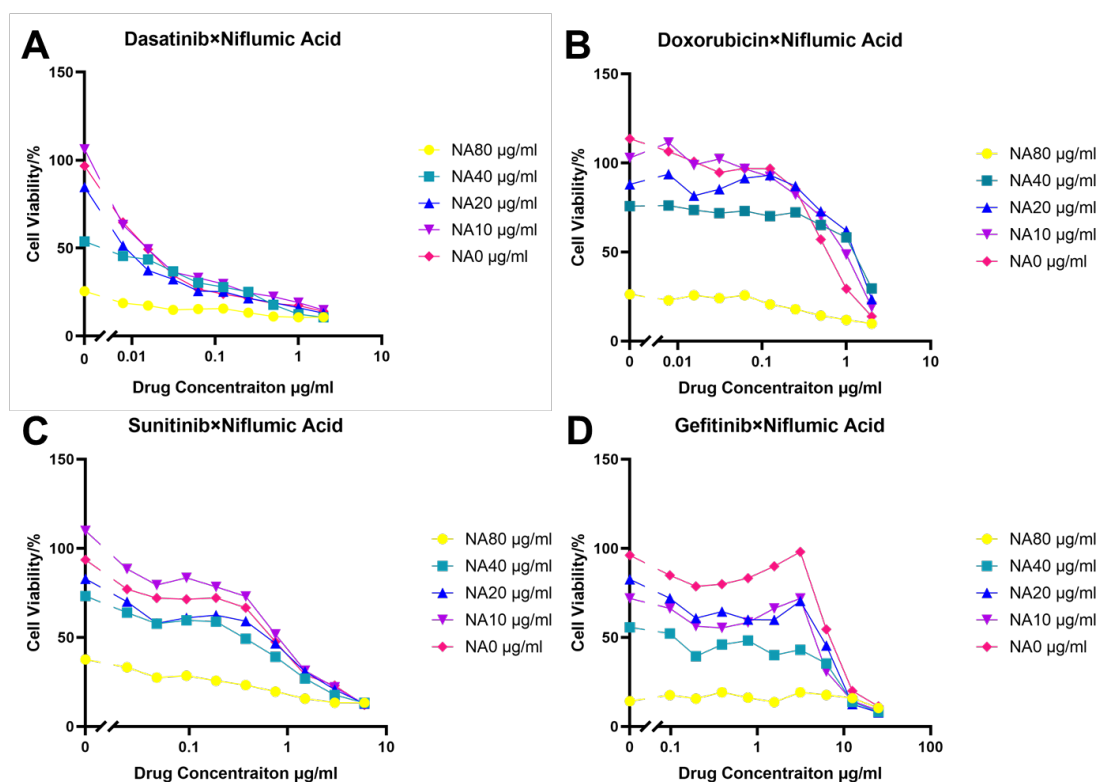
Figure 5 Synergistic effect between NA and dasatinib, doxorubicin, sunitinib or gefitinib in inhibiting the proliferation of 4T1.2 cancer cells

4T1.2 cells were treated with various concentration of free dasatinib (A), doxorubicin (B), sunitinib (C) and gefitinib (D), alone or in combination with different concentration of free NA. After 48 h, the live cells were measured by MTT assay and cell viabilities were normalized by control group. Curves

20

were generated by simply connected all dots together and the proliferation inhibitory effect were determined. The experiments were performed in sextuplicate and repeated three times. Data are presented as means ± SD.

Table 2 Synergistic antiproliferative activity of NA and other anti-cancer drugs in 4T1.2 cells

Drug1	Drug2	d_1 (µg/mL)	$IC_{50}1$ (µg/mL)	d_2 (µg/mL)	$IC_{50}2$ (µg/mL)	CI
Niflumic Acid	Dasatinib	20	50.55	0.0047	0.01389	0.73
Niflumic Acid	Doxorubicin	20	50.55	1.100	0.6184	2.17
Niflumic Acid	Gefitinib	20	50.55	1.845	7.185	0.65
Niflumic Acid	Sunitinib	20	50.55	1.206	2.126	0.96

Combination Index (CI) of simultaneous treatment of NA and other anti-cancer drugs in 4T1.2 cells were calculated. Cells were treated as described in Fig. 5. The anti-proliferation data for single drug and combination treatment were fitted to an inhibitory, normalized dose-response model with variable slope (Y = 100/ (1 + 10^((LogEC50-X) *Hillslope) to calculate their IC_{50} value. Then the CI value was calculated by the formula: CI = (d1/IC501) +(d2/IC502). The CI values are interpreted as follows: <1.0, synergism; 1.0, additive; and >1.0, antagonism.

3.4 Biodistribution of POEG-b-PNA micelles

The biodistribution of POEG-b-PNA micelles after systemic administration was investigated by *in vivo* biofluorescence imaging. A lipophilic near IR fluorescence dye, carbocyanine DiOC18(7) (DiR), was used for micelle tracing. DiR is weakly fluorescent in water but highly fluorescent in lipid environment, suggesting that it shows strong fluorescence when loaded in POEG-b-PNA micelles but becomes minimally fluorescent upon release into blood. Therefore, by loading DiR into POEG-b-PNA micelles, the biodistribution of POEG-b-PNA micelles can be followed by near infrared imaging. As shown in Fig. 6A, strong fluorescence signal was observed for DiR loaded in POEG-b-PNA micelles while free DiR showed a minimal signal, validating the use of DIR to follow the fate of micelle in vivo. The DiR signal was observed at tumor site as early as 1 h after injection, and it remained in tumor even after 72 h, suggesting its long-lasting tumor-targeting effect. After 72 h, mice were sacrificed, and tumors and other organs were taken for *ex vivo* imaging (Figure. 6B-C). In consistent with whole body imaging, signals observed in tumor tissues were significantly higher than those in other tissue and organs, further confirming the selective tumor accumulation of our micelles.
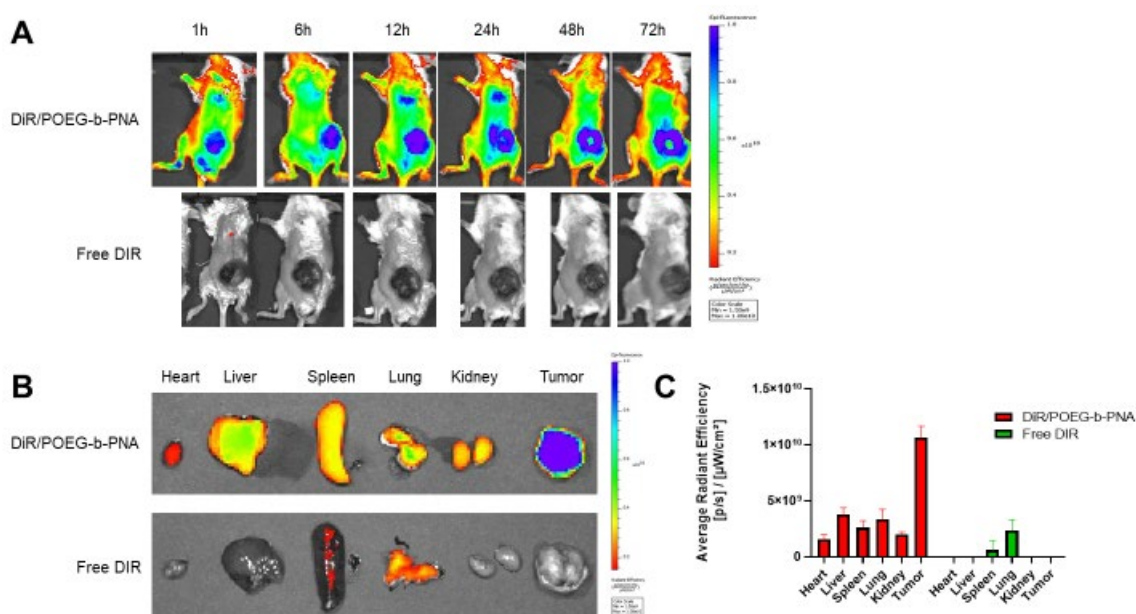
Figure 6 In vivo and ex vivo NIRF imaging of POEG-b-PNA micelles

4T1.2 tumor bearing mice were intravenously injected with free DiR or DiR loaded POEG-b-PNA. After 1, 6, 12, 24, 48 and 72 h, the whole-body fluorescent images were taken (A). Then mice were sacrificed for *ex vivo* organ fluorescent images (B). Fluorescent intensities of different organs at 72 h after injection were quantified (C). Values reported are the means ± SEM, n = 3.

3.5 *In vivo* tumor-inhibitory effect of anti-cancer drugs loaded POEG-b-PNA micelles

Our POEG-b-PNA micelles are capable of formulating various anticancer agents including dasatinib, doxorubicin, sunitinib, and gefitinib. It is well known that the outcome of an in vitro study may not always well correlate with that of an in vivo assay with respect to the antitumor activity of a given therapeutics, particularly a combination therapy. To facilitate the identification of a promising POEG-b-PNA-based combination therapy that warrants more studies later on, a preliminary study was conducted to examine the antitumor activity of various POEG-b-PNA formulations each loaded with a different drug. To start, highly aggressive syngeneic 4T1.2 murine breast cancer cells were injected subcutaneously at mammary fat pad of female mice. Five days later, when solid tumors were noticeable, POEG-b-PNA micelles loaded with dasatinib, doxorubicin, sunitinib or gefitinib were administered intravenously. As shown in Fig. 7A, blank POEG-b-PNA micelles showed minimal anti-tumor activity, this might be due to the modest potency of NA and the limited dose of POEG-b-PNA that was used for codelivery. POEG-b-PNA micelles loaded with Gefitinib or sunitinib also showed no significant difference from control group, possibly because of insufficient cytotoxicity and lack of synergistic effect with NA in vivo. POEG-b-PNA loaded with DOX exhibited significant inhibition on tumor growth, despite lack of

synergy between NA and DOX in MTT assay. However, body weights of mice in this group decreased dramatically, suggesting significant toxicity (Fig. 7B). POEG-b-PNA loaded with dasatinib showed an antitumor activity that was comparable to that of DOX-loaded micelles. However, dasatinib-loaded POEG-b-PNA micelles were well tolerated in treated mice as shown by minimal changes in body weights.
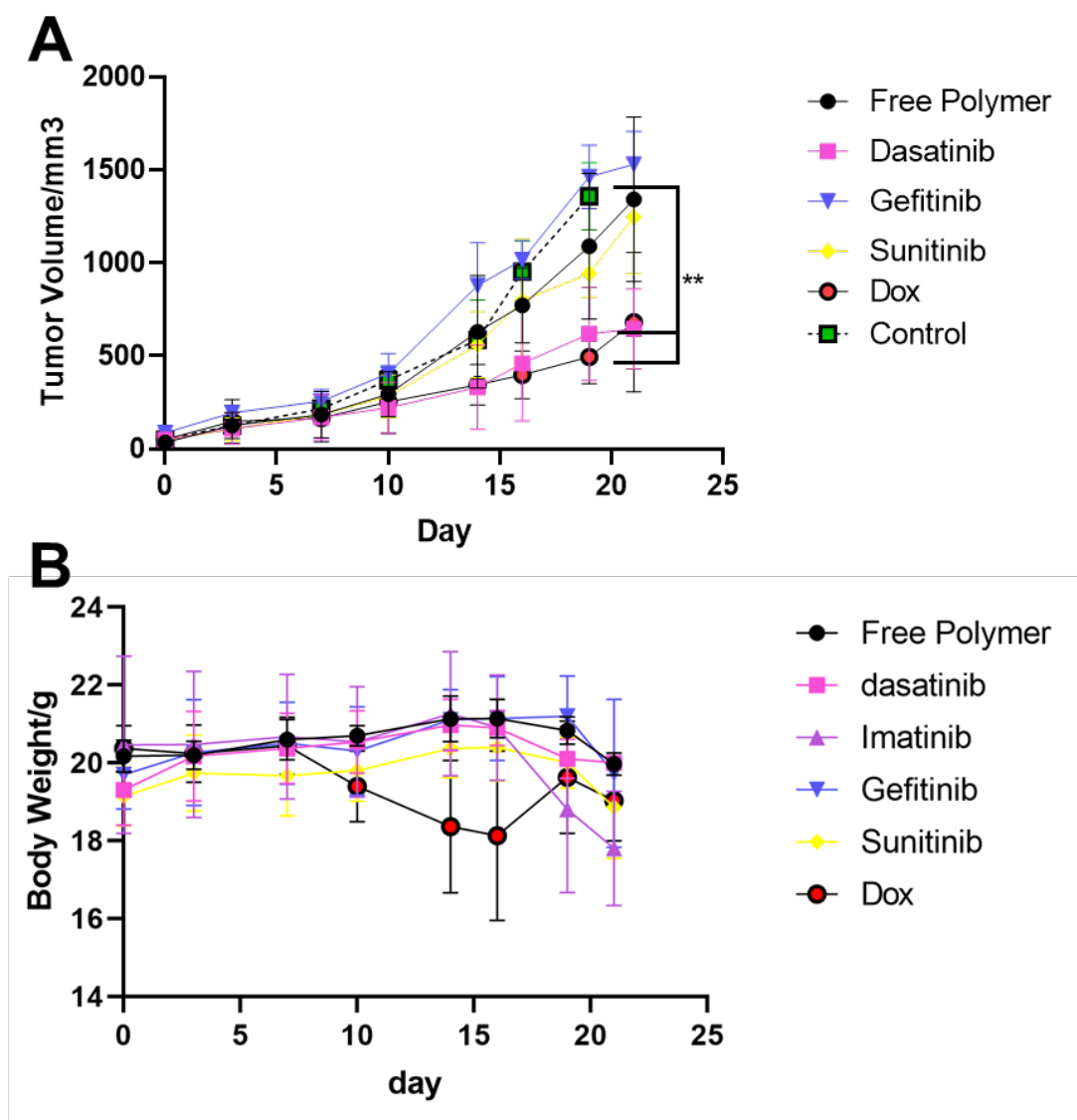
Figure 7 Tumor suppression effect of drug loaded POEG-b-PNA polymers in vivo

All mice were inoculated with 4T1.2 cells 5 days before treatment. Free POEG-b-PNA micelles or micelles loading dasatinib, gefitinib or sunitinib were injected intravenously on day 0, 3, 7, 10 and 14. Doxorubicin (Dox) loaded POEG-b-PNA micelles were given three times on day 0, 3 and 7 because of the decrease body weight. Tumor volume (A) and body weight of (B) mice were followed for 3 weeks.

24

Widths and lengths of tumors were measured, and tumor volumes were calculated according to the equation: Tumor Volume $(mm^3) = \pi*$Length (mm)*Width (mm)*Width (mm)/6. Values reported are the means $\pm$ SEM, n = 3. P values were generated by student t-test for comparisons. *P < 0.05, **P < 0.01 (vs control).

3.6 *In vitro* cytotoxicity of dasatinib loaded POEG-b-PNA micelles

Since dasatinib-loaded POEG-b-PNA showed a significant growth-inhibitory effect in 4T1.2 tumor, further study was conducted to investigate the pharmacokinetic and pharmacodynamic profile of this combination therapy. With the concerns that drugs may not be well released to achieve an effect as effectively as free drugs when they are loaded into micelles, an *in vitro* cytotoxicity of dasatinib-loaded POEG-b-PNA micelles was first tested on 4T1.2 cells and compared to free NA and dasatinib combination. As shown in Fig. 8, dasatinib inhibited the proliferation of 4T1.2 cancer cells in a concentration-dependent manner and the addition of free NA further enhanced this inhibitory activity. Compared with free drug combination, dasatinib-loaded POEG-b-PNA micelles were found to achieve a similar level of cytotoxicity, suggesting that loading into POEG-b-PNA minimally impacted the cytotoxicity of dasatinib. In addition, POEG-b-PNA micelles displayed a reduced cytotoxicity compared with free NA, possibly due to the slow release of NA from micelles.
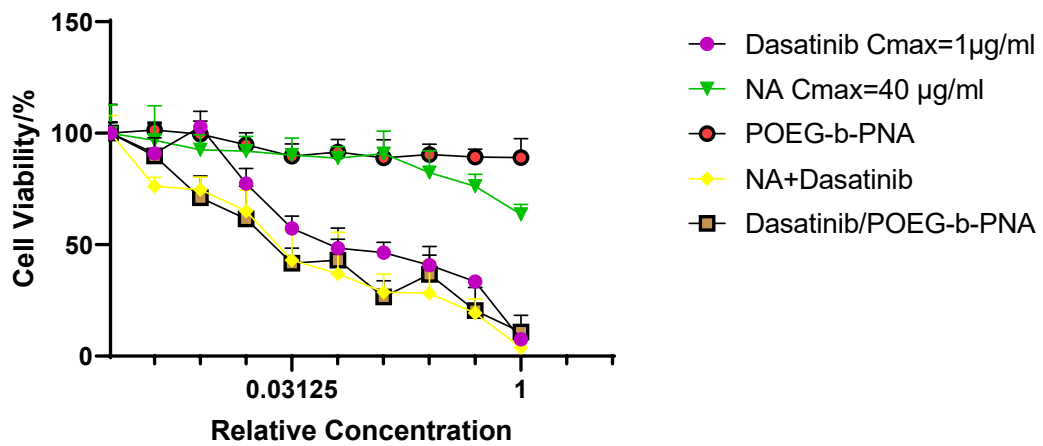
Figure 8 In vitro proliferation inhibitory effect of dasatinib loaded POEG-b-PNA micelles

4T1.2 cells were treated with various concentration of free dasatinib, free NA, free POEG-b-PNA micelles, free dasatinib/NA combination or dasatinib loaded POEG-b-PNA micelles. A same maximum concentration of 1 μg/ml was shared in all dasatinib-including groups. A same maximum concentration of 40 μg/ml was shared in all NA-including groups. After 48 h, the live cells were measured by MTT assay and the proliferation inhibitory effect were determined. The experiments were performed in sextuplicate and repeated three times. Data are presented as means ± SD.

4.0 Discussion

NA, a cyclooxygenase-2 (Cox-2) inhibitor, was first approved by FDA for joint and muscular pain treatment. Recently it was found to be a TEAD-YAP inhibitor targeting the central pocket in human TEAD[27]. Since few direct YAP/TAZ inhibitors have been developed[35], the discovery of NA is exciting because it provides the possibility for researchers to manipulate the Hippo signaling pathway *in vivo* by a small molecule and explore the therapeutic potential of targeting YAP/TAZ. Previously, numerous *in vitro* studies have revealed the important role of YAP/TAZ in cancer cell proliferation, cell survival, cell migration, drug resistance and other essential functions for cancer development. However, little progress was made in the advancement of these studies to *in vivo* evaluations due to the lack of a small molecule inhibitor with an ideal pharmacokinetics/pharmacodynamics profile. NA was found to have a significant inhibition of TEAD-YAP activity in HEK293 cell line[27], but its short half-life of 2.5 h in blood hinders its application *in vivo*. In order to solve this problem, here we developed a NA-based prodrug polymer which shows efficient tumor accumulation for targeted drug delivery. With this polymer, a slow release of NA at tumor site is expected, which shall lead to a sustained inhibition of TEAD-YAP activity for a prolonged period of time. An *in vitro* release study that simulates the *in vivo* release of NA from the polymer and systematic pharmacokinetic study of the prodrug polymer in blood and tissues are underway.

NA was reported to have a high affinity to human TEAD with a K_d of 28 μM [27]. However, a relatively high concentration was required to significantly reduce the expression of the TEAD-YAP target genes as well as the expression of a YAP-luciferase reporter in 4T1.2 cells, indicating an insufficient potency of NA. There are several possible reasons for this discrepancy: First, although the Hippo pathway is highly

conserved, the subtle differences between the structures of human and murine TEAD and YAP/TAZ might account for the discrepancy; Second, though NA decreases TEAD-YAP activity by binding to the central pocket in TEAD, TEAD can still form complex with YAP/TAZ[27], indicating that the activity of this complex is not completely abolished with NA binding and that a concentration that is much higher than its K_d is required to inhibit the TEAD-YAP activity. Therefore, a considerably high concentration is required to inhibit TEAD-YAP activity using NA alone for cancer treatment, which is almost impossible to achieve and maintain *in vivo*. Taking this into account, our POEG-b-PNA polymer was developed for tumor-targeted delivery of NA to increase local drug concentration and other anti-cancer drugs were co-delivered with this system to improve the efficacy through a synergistic action. Interestingly, the *in vitro* MTT showed synergistic effect between dasatinib and NA even at relatively low NA concentrations. In addition, preliminary data showed that codelivery of NA and dasatinib via POEG-b-PNA polymer also led to a better overall antitumor activity *in vivo* compared to other combination therapies. As dasatinib also exhibited YAP-inhibitory effect by indirectly phosphorylating YAP/TAZ thus reducing their nuclear localization[36], the cooperation between NA and dasatinib in YAP inhibition might explain the mechanism behind their synergistic effect.

While YAP/TAZ activity is inhibited by NA, the function of several other cofactors sharing the same pocket in TEAD with YAP/TAZ may also be influenced. Studies showed that the Vestigial-like (VGLL) protein family proteins compete with YAP/TAZ for TEAD binding because of overlapped binding sites[37, 38]. Interestingly, though VGLL1 and VGLL4 both compete with YAP/TAZ, they displayed opposing effect on cell growth as VGLL4 overexpression suppresses tumor growth[37, 39] while VGLL1 promotes anchorage-independent cell growth via a mechanism different from that of YAP/TAZ[38]. Considering the fact that NA does not prevent the formation of TEAD-YAP complex, the effect of NA on YAP/TAZ activity is unexpectedly complex and profound. The selectivity of NA as a YAP inhibitor warrants more studies in the future.

5.0 Conclusion

In 4T1.2 cells with a high expression level of YAP, NA significantly reduced YAP reporter activity and the expression of its target genes without affecting the YAP expression at protein level, which indicates its direct inhibition of YAP. Moreover, strong synergistic effect was observed when 4T1.2 cancer cells were treated with NA in combination with dasatinib or gefitinib.

In addition, we have developed a well-characterized POEG-b-PNA prodrug-based micellar nanocarrier that consists of 13 units of PNA and 14 units of POEG for efficient delivery of water insoluble anticancer drugs. This micelle has a small size of about 10 nm, which enables it to penetrate deeply into tumor. At the same time, the critical micelle concentration is very low, suggesting that it is stable and not easy to disassemble following i.v. administration. Furthermore, its ability to accumulate at tumor site was verified by biodistribution study, suggesting that NA and hydrophobic drug can be efficiently co-deliver to tumor. Last, this strategy was proved to significantly suppress tumor growth in 4T1.2 tumor-bearing mice.

Bibliography

[1] R. Johnson, G. Halder, The two faces of Hippo: targeting the Hippo pathway for regenerative medicine and cancer treatment, Nature reviews Drug discovery 13(1) (2014) 63-79.

[2] J.S. Mo, H.W. Park, K.L. Guan, The Hippo signaling pathway in stem cell biology and cancer, EMBO reports 15(6) (2014) 642-656.

[3] K.F. Harvey, X. Zhang, D.M. Thomas, The Hippo pathway and human cancer, Nature Reviews Cancer 13(4) (2013) 246.

[4] N. Tapon, K.F. Harvey, D.W. Bell, D.C. Wahrer, T.A. Schiripo, D.A. Haber, I.K. Hariharan, salvador Promotes both cell cycle exit and apoptosis in Drosophila and is mutated in human cancer cell lines, Cell 110(4) (2002) 467-478.

[5] T. Xu, W. Wang, S. Zhang, R.A. Stewart, W. Yu, Identifying tumor suppressors in genetic mosaics: the Drosophila lats gene encodes a putative protein kinase, Development 121(4) (1995) 1053-1063.

[6] R.W. Justice, O. Zilian, D.F. Woods, M. Noll, P.J. Bryant, The Drosophila tumor suppressor gene warts encodes a homolog of human myotonic dystrophy kinase and is required for the control of cell shape and proliferation, Genes & development 9(5) (1995) 534-546.

[7] I.M. Moya, G. Halder, Hippo–YAP/TAZ signalling in organ regeneration and regenerative medicine, Nature Reviews Molecular Cell Biology 20(4) (2019) 211-226.

[8] M. Praskova, F. Xia, J. Avruch, MOBKL1A/MOBKL1B phosphorylation by MST1 and MST2 inhibits cell proliferation, Current Biology 18(5) (2008) 311-321.

[9] B.A. Callus, A.M. Verhagen, D.L. Vaux, Association of mammalian sterile twenty kinases, Mst1 and Mst2, with hSalvador via C-terminal coiled-coil domains, leads to its stabilization and phosphorylation, The FEBS journal 273(18) (2006) 4264-4276.

[10] S. Wu, J. Huang, J. Dong, D. Pan, hippo encodes a Ste-20 family protein kinase that restricts cell proliferation and promotes apoptosis in conjunction with salvador and warts, Cell 114(4) (2003) 445-456.

[11] Y. Hao, A. Chun, K. Cheung, B. Rashidi, X. Yang, Tumor suppressor LATS1 is a negative regulator of oncogene YAP, Journal of Biological Chemistry 283(9) (2008) 5496-5509.

[12] Q.-Y. Lei, H. Zhang, B. Zhao, Z.-Y. Zha, F. Bai, X.-H. Pei, S. Zhao, Y. Xiong, K.-L. Guan, TAZ promotes cell proliferation and epithelial-mesenchymal transition and is inhibited by the hippo pathway, Molecular and cellular biology 28(7) (2008) 2426-2436.

[13] B. Zhao, X. Wei, W. Li, R.S. Udan, Q. Yang, J. Kim, J. Xie, T. Ikenoue, J. Yu, L.

Li, Inactivation of YAP oncoprotein by the Hippo pathway is involved in cell contact inhibition and tissue growth control, Genes & development 21(21) (2007) 2747-2761.

[14] C.-Y. Liu, Z.-Y. Zha, X. Zhou, H. Zhang, W. Huang, D. Zhao, T. Li, S.W. Chan, C.J. Lim, W. Hong, The hippo tumor pathway promotes TAZ degradation by phosphorylating a phosphodegron and recruiting the SCFβ-TrCP E3 ligase, Journal of Biological Chemistry 285(48) (2010) 37159-37169.

[15] B. Zhao, L. Li, K. Tumaneng, C.-Y. Wang, K.-L. Guan, A coordinated phosphorylation by Lats and CK1 regulates YAP stability through SCFβ-TRCP, Genes & development 24(1) (2010) 72-85.

[16] B. Zhao, X. Ye, J. Yu, L. Li, W. Li, S. Li, J. Yu, J.D. Lin, C.-Y. Wang, A.M. Chinnaiyan, TEAD mediates YAP-dependent gene induction and growth control, Genes & development 22(14) (2008) 1962-1971.

[17] D. Lai, K.C. Ho, Y. Hao, X. Yang, Taxol resistance in breast cancer cells is mediated by the hippo pathway component TAZ and its downstream transcriptional targets Cyr61 and CTGF, Cancer research 71(7) (2011) 2728-2738.

[18] Z. Meng, T. Moroishi, K.-L. Guan, Mechanisms of Hippo pathway regulation, Genes & development 30(1) (2016) 1-17.

[19] S.W. Chan, C.J. Lim, L.S. Loo, Y.F. Chong, C. Huang, W. Hong, TEADs mediate nuclear retention of TAZ to promote oncogenic transformation, Journal of Biological Chemistry 284(21) (2009) 14347-14358.

[20] H. Song, K.K. Mak, L. Topol, K. Yun, J. Hu, L. Garrett, Y. Chen, O. Park, J. Chang, R.M. Simpson, Mammalian Mst1 and Mst2 kinases play essential roles in organ size control and tumor suppression, Proceedings of the National Academy of Sciences 107(4) (2010) 1431-1436.

[21] J.M. Lamar, P. Stern, H. Liu, J.W. Schindler, Z.-G. Jiang, R.O. Hynes, The Hippo pathway target, YAP, promotes metastasis through its TEAD-interaction domain, Proceedings of the National Academy of Sciences 109(37) (2012) E2441-E2450.

[22] M. Cordenonsi, F. Zanconato, L. Azzolin, M. Forcato, A. Rosato, C. Frasson, M. Inui, M. Montagner, A.R. Parenti, A. Poletti, The Hippo transducer TAZ confers cancer stem cell-related traits on breast cancer cells, Cell 147(4) (2011) 759-772.

[23] A. Fernandez-L, M. Squatrito, P. Northcott, A. Awan, E.C. Holland, M.D. Taylor, Z. Nahlé, A.M. Kenney, Oncogenic YAP promotes radioresistance and genomic instability in medulloblastoma through IGF2-mediated Akt activation, Oncogene 31(15) (2012) 1923-1937.

[24] L. Lin, A.J. Sabnis, E. Chan, V. Olivas, L. Cade, E. Pazarentzos, S. Asthana, D. Neel, J.J. Yan, X. Lu, The Hippo effector YAP promotes resistance to RAF-and MEK-targeted cancer therapies, Nature genetics 47(3) (2015) 250-256.

[25] G. Halder, R.L. Johnson, Hippo signaling: growth control and beyond, Development 138(1) (2011) 9-22.

[26] T. Moroishi, C.G. Hansen, K.-L. Guan, The emerging roles of YAP and TAZ in cancer, Nature Reviews Cancer 15(2) (2015) 73-79.

[27] A.V. Pobbati, X. Han, A.W. Hung, S. Weiguang, N. Huda, G.Y. Chen, C. Kang, C.S. Chia, X. Luo, W. Hong, A. Poulsen, Targeting the Central Pocket in Human Transcription Factor TEAD as a Potential Cancer Therapeutic Strategy, Structure 23(11) (2015) 2076-86.

[28] A.V. Pobbati, W. Hong, Emerging roles of TEAD transcription factors and its coactivators in cancers, Cancer biology & therapy 14(5) (2013) 390-398.

[29] G. Houin, D. Tremblay, F. Bree, A. Dufour, P. Ledudal, J. Tillement, The pharmacokinetics and availability of niflumic acid in humans, International journal of clinical pharmacology, therapy, and toxicology 21(3) (1983) 130-134.

[30] S. Dupont, L. Morsut, M. Aragona, E. Enzo, S. Giulitti, M. Cordenonsi, F. Zanconato, J. Le Digabel, M. Forcato, S. Bicciato, Role of YAP/TAZ in mechanotransduction, Nature 474(7350) (2011) 179-183.

[31] Z. Li, J. Sun, Y. Huang, Y. Liu, J. Xu, Y. Chen, L. Liang, J. Li, Q. Liao, S. Li, A Nanomicellar Prodrug Carrier Based on Ibuprofen-Conjugated Polymer for Co-delivery of Doxorubicin, Frontiers in pharmacology 9 (2018) 781.

[32] X. Huo, Q. Zhang, A.M. Liu, C. Tang, Y. Gong, J. Bian, J.M. Luk, Z. Xu, J. Chen, Overexpression of Yes-associated protein confers doxorubicin resistance in hepatocellullar carcinoma, Oncology reports 29(2) (2013) 840-846.

[33] C. Wang, H. Huang, T.-y. Hong, Y.-n. Wang, Y. Li, C.-m. Chu, J. Zhang, X.-w. Pan, C.-y. Hu, J.-c. Zheng, Degalactotigonin Exerts Effective Inhibition on the Growth, Metastasis and Sunitinib-Resistance of Renal Cell Carcinoma Through Inactivating YAP Signaling, (2018).

[34] J.E. Lee, H.S. Park, D. Lee, G. Yoo, T. Kim, H. Jeon, M.-K. Yeo, C.-S. Lee, J.Y. Moon, S.S. Jung, Hippo pathway effector YAP inhibition restores the sensitivity of EGFR-TKI in lung adenocarcinoma having primary or acquired EGFR-TKI resistance, Biochemical and biophysical research communications 474(1) (2016) 154-160.

[35] W.C. Juan, W. Hong, Targeting the Hippo signaling pathway for tissue regeneration and cancer therapy, Genes 7(9) (2016) 55.

[36] J. Rosenbluh, D. Nijhawan, A.G. Cox, X. Li, J.T. Neal, E.J. Schafer, T.I. Zack, X. Wang, A. Tsherniak, A.C. Schinzel, β-Catenin-driven cancers require a YAP1 transcriptional complex for survival and tumorigenesis, Cell 151(7) (2012) 1457-1473.

[37] S. Jiao, H. Wang, Z. Shi, A. Dong, W. Zhang, X. Song, F. He, Y. Wang, Z. Zhang, W. Wang, A peptide mimicking VGLL4 function acts as a YAP antagonist therapy against gastric cancer, Cancer cell 25(2) (2014) 166-180.

[38] Ajaybabu V. Pobbati, Siew W. Chan, I. Lee, H. Song, W. Hong, Structural and Functional Similarity between the Vgll1-TEAD and the YAP-TEAD Complexes, Structure 20(7) (2012) 1135-1140.

[39] W. Zhang, Y. Gao, P. Li, Z. Shi, T. Guo, F. Li, X. Han, Y. Feng, C. Zheng, Z. Wang, F. Li, H. Chen, Z. Zhou, L. Zhang, H. Ji, VGLL4 functions as a new tumor suppressor in lung cancer by negatively regulating the YAP-TEAD transcriptional

complex, Cell Research 24(3) (2014) 331-343.